Nominal and Effective Volume Fractions in Polymer−Clay Nanocomposites

Biqiong Chen and Julian R. G. Evans*

Department of Materials, Queen Mary, University of London, Mile End Road, London E1 4NS, United Kingdom

Received October 18, 2005; Revised Manuscript Received January 12, 2006

ABSTRACT: This paper aims to clarify the calculation of effective phase volume fractions in polymer−clay nanocomposites so that conventional composite theory for the volume fraction dependencies of properties can be applied. In this way, such nanocomposites, which are treated as a separate class of composites, can be brought under the umbrella of general composite theory so that property predictions and formulation decisions can have a wider theoretical base. Intercalation results in the expansion of the dispersed phase and absorption of the continuous phase so that the reinforcing unit is itself a composite. In exfoliation, a high surface area of dispersed phase is presented to the continuous phase with consequences for adsorption and immobilization. Many nanocomposites are a mixture of these two modes for which a theoretical expression is also needed.

I. Introduction

The definition of a composite material that emerges from Hull's text[1] is of two or more physically distinct and mechanically separable materials mixed in such a way that the dispersion of one material in the other is controlled to achieve optimum properties that are superior to the properties of the individual components. The IUPAC specification[2] defines a composite as "a multicomponent material comprising multiple different (nongaseous) phase domains in which at least one type of phase domain is a continuous phase". A nanocomposite is defined as "a composite in which at least one of the phases has at least one dimension of the order of nanometres". A continuous or matrix phase domain is further defined as "a phase domain consisting of a single phase in a heterogeneous mixture through which a continuous path to all phase domain boundaries may be drawn without crossing a phase domain boundary".

In polymer−clay nanocomposites, physical distinction is blurred as a result of mixing at a molecular level during intercalation, mechanical separation is no longer always possible, and the intercalation process is not yet directly controllable. It may become partially controllable by exchange of cations, adsorption inter alia of ammonium compounds, and adjustment of concentrations and reaction times and by the judicious use of copolymers. Even so, the physical properties of the individual phases may change when mixing takes place at a molecular level; the polymer, for example, cannot be treated as a continuum if confined or immobilized segments present a high volume fraction or bridging molecules interact with more than one dispersoid. Both become possible when the radius of gyration is of the same order as the dimension of the dispersoids.

The properties of binary composites are usually interpreted in terms of the volume fractions of the physically distinct phases. Thus, a large collection of elastic modulus−volume fraction relationships have been devised for particle reinforced conventional composites, e.g., refs 3−5. Similarly, thermal properties,[6] dielectric properties,[7] permeation properties,[8] and other transport properties[9] are related to volume fraction and to the geometry of the dispersed phase. A newer approach to such composites attempts to relate properties not just to volume fraction but to contiguity and hence continuous volume fraction of the dispersed phase, thus subsuming the many simple volume fraction relationships but requiring additional quantitative microstructural information,[10] some of which might be deduced from electron microscope images.

The outstanding feature of polymer−clay nanocomposites is the claim that property enhancements are obtained at much lower particle loadings (1−10 wt %) than would be needed in conventional composites (20−40 wt %). Yano et al.[11] stated "In general, to reinforce a polymer, 20−30 wt % of inorganic materials (glass fiber, talc, etc.) are used. As for clay, about one-tenth that amount is enough to improve the properties of a matrix polymer". Thus, Kojima et al.[12] claim that "NCH (Nylon 6−clay hybrid, montmorillonite: 4.7 wt %) at 120 °C has a flexural strength more than double and a flexural modulus four times that of nylon 6. Yet NCH has an impact strength comparable to nylon 6. HDT, an index of heat resistance, increases from 65 °C to 152 °C" and "at 120 °C, the tensile modulus of NCH is three times that of nylon 6". Lan and Pinnavaia[13] claim "more than a 10-fold increase in strength and modulus is realized by the addition of only 15 wt % (∼7.5 vol %) of exfoliated organoclay". Wang and Pinnavaia[14] find that at a loading of only 10 wt % (∼5 vol %) organoclay the tensile strength, modulus, and strain at break all increased by more than 100%. Yano et al.[15] observe that at 2 wt % clay loading (∼1 vol %), the permeability coefficient of water vapor was decreased 10-fold for the synthetic fluorohectorite relative to pristine polyimide. They also found that "only 2 wt % addition of montmorillonite brought gas permeability to value less than half of that of polyimide".[11]

Do these dramatic property enhancements mean that nanocomposites violate composite theory? Does a nanocomposite modulus really exceed that predicted by the volumetric law of mixtures? It is not easy to tell for several reasons. When the clay intercalates, it not only expands, thus increasing its own volume fraction, but also absorbs polymer thus decreasing the volume of dispersed phase. It appears from the literature[16] that the clay can present the same expanded structure as witnessed by increased spacing of the basal (001) plane over a wide range of absorption. The effective density of the dispersed phase may

* To whom correspondence should be addressed. E-mail: j.r.g.evans@qmul.ac.uk.

10.1021/ma0522460 CCC: $33.50
Published on Web 02/09/2006

thus be reduced not just by absorption of polymer with a density typically one-third but also because the polymer does not exert its bulk density in the galleries.

When the clay exfoliates, the clay volume fraction decreases because of the loss of interplanar spacing. However, its contact area with polymer increases dramatically to its total surface area (from ∼40 to ∼760 $m^2\ g^{-1}$ for montmorillonites as calculated from structure),[17,18] and the polymer adsorbed on its surface is increased by the same factor. Does the large interfacial area play a role in improving properties by restricting segment mobility, and does the adsorbed polymer significantly increase the effective volume fraction of solid, an effect well-known in conventional polymer composites employing fine particles?[19,20]

These, of course, are not the only problems. The polymer in the galleries is strongly adsorbed on adjacent plates and likely to exert a different modulus than the bulk. Similarly the clay platelets, acting as a reinforcing phase in their own right, exert a higher modulus than the tactoids because the weak interplanar bonding is absent. The clay tactoids are sufficiently fine to have interparticle spacings that allow a polymer tie chain network to develop providing a kind of physical cross-linking through adsorption. Platelets dispersed in a semicrystalline polymer may increase polymer crystallinity,[21,22] and intercalated polymer may lose its folding ability.[23−25] Finally, the arrangements of high aspect ratio platelets, particularly if preferred orientation is present, provide a high level of tortuosity to gaseous diffusers or permeants.

II. Theory

A. Conventional Composites. In a conventional binary polymer−clay composite the volume fraction of the dispersed phase is given by

$$1/\phi_c = 1 + \rho_c(1 - \mu_c)/\rho_p\mu_c \tag{1}$$

where ρ is density and μ is mass fraction. The subscripts c and p refer to clay and polymer. No ambiguity attends this calculation unless the particle size is sufficiently small that polymer adsorption contributes to the effective volume fraction of the dispersed phase. The adsorbed layer is typically similar to the radius of gyration of the polymer R_g[26−28] so the volume of clay must be increased by $R_gA_p\rho_c$, giving an increased effective clay volume fraction, ϕ_c'

$$\phi_c' = \phi_c(1 + R_gA_p\rho_c) \tag{2}$$

where A_p is the specific particle surface area. Thus, for a clay with specific surface area 38 $m^2\ g^{-1}$ and density 2600 kg m^{-3}, a polymer with radius of gyration 10 nm effectively doubles the volume fraction of dispersed phase. In fact, only a fraction of the adsorbed layer, *k*, would behave as solid, and mechanical testing or viscosity measurement can be used to estimate this fraction. So eq 2 becomes

$$\phi_c' = \phi_c(1 + kR_gA_p\rho_c) \tag{3}$$

As the specific surface area of a clay particle is comparable to other particulate reinforcements, most conventional composites containing a low volume fraction of clay present limited modulus enhancement. If the nanocomposite is exfoliated, the full experimental specific surface area of clay, 658 $m^2\ g^{-1}$,[29] applies (vide infra).

B. Intercalated Nanocomposites. *1. Intercalated Tactoids of Untreated Clay.* In intercalated nanocomposites, polymer molecules enter into clay galleries, increasing the basal plane spacing from d_1 to d_2, as shown in Figure 1. This diagram shows an idealized intercalation morphology in which all the polymer molecules are intercalated into clay galleries and gallery water is displaced; i.e., there is no excess (interstitial) polymer between clay particles. The specific gallery area, *A*, is obtained from the total specific surface area, A_T, by subtracting A_p and noting that there are two surfaces per gallery, $A = (A_T - A_p)/2$. Referring to Figure 1 which shows the intercalation reaction with a corresponding increase in basal plane spacing, the volume fraction of clay platelets is

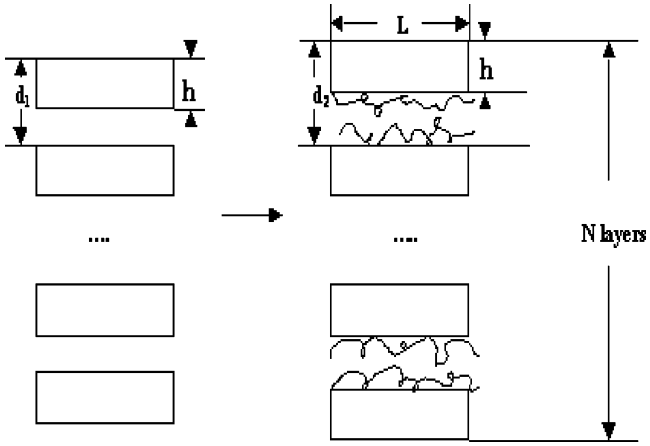

Figure 1. Schematic diagram of intercalation.

$$\phi_c = \frac{hN}{d_2(N-1) + h} \tag{4}$$

If the number of platelets in a tactoid, *N*, is large, this reduces to $\phi_c \approx h/d_2$. For typical values of $h = 0.98$ nm and $d_2 = 1.7$ nm, reinforcing tactoids must have more than eight platelets to incur an error of less than 5% using the reduced equation. Indeed, they often have less than eight platelets.

If the intercalated polymer occupies the whole available space in the interlayer of clay, the fraction of polymer is

$$\phi_p = \frac{(d_2 - h)(N-1)}{d_2(N-1) + h} \tag{5}$$

This can be reduced to $\phi_p \approx (d_2 - h)/d_2$ if $N > 11$ to keep the error below 5%.

The validity of this calculation using clay surface area is easily deduced. The basal plane spacing of the natural montmorillonite is 1.23 nm as measured by XRD.[17] The normalized experimental value of the total specific surface area of montmorillonite is 658 $m^2\ g^{-1}$ as noted before, and the external specific surface area measured by BET N_2 adsorption is 38 $m^2\ g^{-1}$,[17] so the internal specific surface area is 620 $m^2\ g^{-1}$. The specific gallery area is thus 310 $m^2\ g^{-1}$. The specific volume of the natural clay is thus $A[d_1(N-1) + h]/(N-1) \approx 310 \times 1.23 = 3.81 \times 10^{-4}$ $m^3\ kg^{-1}$ as *N* is sufficiently large (equal to 813 if the particle size of clay is 1 μm) to neglect the effect of *h*; the error is then 0.1%. The specific volume obtained from the measured density ($\rho_c = 2.6 \times 10^3$ kg m^{-3}) is 3.84×10^{-4} kg m^{-3}. These values agree to 1%, so this calculation is valid and precise.

This approach does not take account of the fact that X-ray diffraction studies combined with measurements of polymer uptake suggest that the basal plane spacing can remain constant over a range of uptakes, implying that the polymer in the gallery does not exert its bulk density. The value of the density exerted

by the intercalated polymer can be found by carrying out the intercalation, adopting a washing protocol to remove the interstitial polymer (that between particles), and then conducting a loss on ignition for residual polymer. By considering only the intercalated clay tactoids, the intercalated mass fraction of polymer is $1 - \mu_c^i$ and the effective polymer density is

$$\rho_p^e = \frac{2(1-\mu_c^i)}{\mu_c^i(d_2 - h)(A_T - A_p)} \tag{6}$$

Noting that for this type of composite all the clay is intercalated and so $\mu_c = \mu_c^i$.

For large tactoids, this can be expressed as

$$\rho_p^e = \frac{s\rho_c d_1}{d_2 - h} \tag{7}$$

since $\rho_c = 2/d_1(A_T - A_P)$.

The uptake of polymer s is generally expressed as mass of polymer intercalated into unit mass of clay and is therefore $(1 - \mu_c^i)/\mu_c^i$ based on the mass of intercalated tactoids. A typical experimental uptake of poly(ethylene glycol) (PEG1500) was 0.23 g per g of clay ($\mu_c^i = 0.81$), giving rise to a basal plane spacing of 1.82 nm.[30] After correction for polymer absorbed on the outer surfaces,[17] the galleries hosted 0.18 g per g of clay ($\mu_c^i = 0.85$). The collapsed layer has a spacing of 0.98 nm ($h =$ 0.98 nm), and the total specific gallery area is 310 $m^2\ g^{-1}$. The effective polymer density is thus 678 kg m^{-3}, and in this case, the polymer exerts less than its bulk density 1130 kg m^{-3}. When the intercalation achieves equilibrium, the intercalation amount corresponds to an uptake of 0.5 g g^{-1} clay and after correction for adsorption 0.39 g g^{-1} clay ($\mu_c^i = 0.72$).

The effective polymer density is thus 1493 kg m^{-3}, suggesting either tighter packing or that an additional 13% polymer is edge intercalated by sufficient number of segments to be firmly attached to the clay edges and cannot be removed by extraction treatments. This edge attachment may be only partially accounted for by the correction made for particle surface adsorption which is based on an average value for the outer surface of clay particles either of kaolinite or of heat-treated montmorillonite which do not intercalate. Thus, specific edge adsorption may be higher than the average surface adsorption because of the entrapment made possible by partial intercalation at the edge of particles. These uptakes agree with the value measured by others, 0.39 g g^{-1} clay for poly(ethylene oxide) with number-average molecular weight of 172 700.[24] Therefore, the effective polymer density in the galleries depends on the preparation conditions.

2. Intercalated Tactoids in Organoclay. According to proposed models for clay that has been pretreated with quaternary ammonium compounds or similar agents (organoclay) to render it accessible by semi- or nonpolar polymers,[31,32] the intercalated polymer occupies the volume provided by the increased basal plane spacing. If the basal plane spacing of the organoclay is d_1', the volume fraction of organoclay in the composite is

$$\phi_c = \frac{d_1'(N-1) + h}{d_2(N-1) + h} \tag{8}$$

This reduces to $\phi_c \approx d_1'/d_2$ if $N > 3$, the condition for a 5% error using typical values of $d_1' = 2$ nm and $d_2 = 2.8$ nm. The volume fraction of polymer is

$$\phi_p = \frac{(d_2 - d_1')(N-1)}{d_2(N-1) + h} \tag{9}$$

simplifying to $\phi_p \approx (d_2 - d_1')/d_2$ for $N > 2$.

Since both surfactant and polymer are present in the clay galleries, they can be treated, to a first-order approximation, as the same phase for the purpose of mechanical property estimation by assuming the surfactant molecules exert the same properties as for polymer. Thus, only the clay platelets are considered as reinforcement. The volume fraction of the clay platelets can be calculated using eq 4.

3. Intercalated Composites with Free Polymer. Thus far, we do not account for the "free" polymer between particles. The intercalated nanocomposite is in fact made up of intercalated clay tactoids and interstitial or "free" polymer between tactoids, as proposed in Figure 2. To describe the interstitial polymer as "free" is probably misleading. The R_g is large enough in comparison with the diameter of tactoids for there to be a tie-chain network, thus limiting segment mobility between clay tactoids. However, the polymer molecules forming tie chains only occupy a small volume fraction of the interstitial polymer, and therefore the tie-chain network is neglected in the following discussions. In this system, it is the intercalated clay tactoids that play the role of reinforcement rather than clay particles.

The total volume of the intercalated nanocomposite is composed of a volume of interstitial polymer V_p^i and a volume of intercalated clay tactoids V_c^i. The absolute volume of the intercalated phase is

$$V_c^i = \frac{\mu_c A[d_2(N-1) + h]}{N-1} \tag{10}$$

and the volume of the "free" polymer is

$$V_p^i = \frac{1 - \mu_c - \mu_c s}{\rho_p} \tag{11}$$

The volume fraction of the intercalated phase $\phi_c^i = V_c^i/(V_c^i + V_p^i)$ and is given by

$$\frac{1}{\phi_c^i} = 1 + \frac{[1 - \mu_c(1+s)](N-1)}{\rho_p \mu_c A[d_2(N-1) + h]} \tag{12}$$

When the number of clay platelets per tactoid is large, this becomes

$$\frac{1}{\phi_c^i} = 1 + \frac{2[1 - \mu_c(1+s)]}{\rho_p \mu_c d_2(A_T - A_p)} \tag{13}$$

By considering the density of the composite ρ, the volume fraction of intercalated reinforcement is

$$\phi_c^i = \frac{\rho\mu_c A[d_2(N-1) + \mathrm{h}]}{N-1} \tag{14}$$

and for large tactoids

$$\phi_c^i = \rho\mu_c d_2(A_T - A_p)/2 \tag{15}$$

Alternatively, by considering the densities of the nanocomposite and the polymer, the volume fraction of free polymer can be expressed as

$$\phi_p^i = \rho[1 - \mu_c(1+s)]/\rho_p \tag{16}$$

Figure 2. Clay stacks acting as the reinforcement filler. The volume inside the broken line can be considered as a single larger platelet.

As an example, the effective volume fraction of clay reinforcement filler in PEG1500−clay nanocomposite prepared by melt-processing[30] is calculated as follows. The nanocomposite consists of 43 wt % polymer and 57 wt % clay. If the same degree of saturation occurs in melt processing as that in solution preparation, 1 g of clay intercalates 0.18 g of PEG. Thus, s in eq 12 is taken as 0.18. The average layer number per stack, N, is deduced from the TEM image as 6. Neglecting the presence of the small amount of single clay platelets, the volume fraction of intercalated clay tactoids is 0.55, in which case the density of polymer is taken as 1130 kg m^{-3}. This value is much higher than the nominal volume fraction of 0.28, suggesting the calculation of effective volume fraction is essential if one wants to interpret properties correctly.

In the case of organoclay, the reinforcement filler is the organoclay intercalated with polymer, namely the intercalated organoclay tactoids. Thus, the effective volume fraction of the reinforcement is given by

$$\frac{1}{\phi_c^i} = 1 + \frac{\rho_c'(1 - \mu_c' - \mu_c'\mu_c^o s)[d_1'(N-1) + h]}{\mu_c'\rho_p[d_2(N-1) + h]} \quad (17)$$

where ρ_c' refers to the density of the organoclay, μ_c' is the mass fraction of the organoclay in the mixture, μ_c^o is the mass fraction of clay platelets in the organoclay, and d_1' is the basal plane spacing of the organoclay.

C. Exfoliated Nanocomposites. Once the clay platelets are dispersed homogeneously in the polymer matrix, the composite can again be treated as a conventional composite for the purpose of finding the phase volume fractions. The main difference from a conventional composite is the adsorption effect. In eq 3, A_p becomes A_T, the total specific surface area of the platelets, and takes the experimental value of 658 m^2 g^{-1} rather than the theoretical value of 760 m^2 g^{-1} which is calculated from the crystalline structure. Also, ρ_c becomes ρ_c^p (the density of clay platelet). As the bulk clay often contains ~6 wt % interlayer water,[30,33] the mass fraction of the platelets in bulk clay is 0.94. The volume fraction of the platelets in bulk clay is 0.98 nm/1.23 nm = 0.80. Thus, the density of the platelets ρ_c^p is 0.94/0.80 × 2600 kg m^{-3} = 3100 kg m^{-3}. Thus eq 3 becomes

$$\phi_c' = \phi_c(1 + kR_gA_T\rho_c^p) \quad (18)$$

Then the effective solid volume fraction is doubled using the same conditions described in the section on conventional composites (i.e., R_g = 10 nm) if k is only 0.05. This goes some way to explaining the strong reinforcing effect of a nanofiller.

In the case of organoclay, the effective volume fraction of exfoliated clay platelets also follows eq 18, but ϕ_c is then $\mu_c'\mu_c^o\rho/\rho_c^p$. To apply eq 18 in real cases, the value of the coefficient k needs to be calculated. In exfoliated nanocomposites, the ammonium molecules are adsorbed on the external surfaces,[34] and since the clay content is often lower than 5 wt %, there is a sufficiently small amount of surfactant to treat it as having the same elastic modulus as the polymer matrix.

Table 1. Effective Volume Fractions of Clay Reinforcement for Nylon-6−Clay Nanocomposites Reported in the Literature[35]

platelets (wt %)	tensile modulus (GPa)	platelets (vol %)	true vol %[a]	k
0	2.75	0	0	
1.6	3.40	0.56	2.6	0.23
3.2	3.92	1.14	4.7	0.20
4.7	4.50	1.69	7.1	0.20
7.2	5.72	2.63	11.9	0.22

[a] Effective volume fractions are deduced using Christensen's model.

Fornes et al.[35] showed that nylon-6 with a molecular weight of 29 300 formed clay nanocomposites with clay contents of 1.6−7.2 wt % that are nearly fully exfoliated, and comprehensive information is given about this system. The density of nylon-6 is 1080 kg m^{-3},[35] and R_g was calculated as 7.8 nm for this nylon-6, based on the bond lengths of C−N of 0.138 nm and C−C of 0.154 nm. A_T = 658 m^2 g^{-1}; thus, $R_gA_T\rho_c^p$ is equal to 15.91.

Christensen's model for randomly dispersed platelet system[36,37] can be selected to express the known Young's modulus of these nanocomposites in terms of their true volume fractions ϕ_c'. By putting these data into eq 18, the values of k can be deduced and are shown in Table 1. Thus, the mean value of k is 0.21 with a standard deviation of 0.015. The true volume fractions ϕ_c' were also deduced using the Mori−Tanaka−Tandon method,[38,39] and the results are very similar to those from Christensen's method, the values of k being 0.24, 0.21, 0.21, and 0.24.

Since the adsorption coefficients obtained from the nylon-6−clay nanocomposites containing different amounts of clay platelets are consistent, eqs 2 and 18 are regarded as valid for the fully exfoliated nanocomposites as well as conventional composites. It should be noted that the value of k depends on the type of polymer and clay.

D. Intercalated−Exfoliated Nanocomposites. According to the literature,[40] most nanocomposites include both intercalated and exfoliated platelets. This kind of nanocomposite should be considered as a mixture of two composites: the intercalated nanocomposite and the exfoliated nanocomposite. Clay platelets act as the reinforcement filler for both nanocomposites. The volume fraction of these two composites in the intercalated−exfoliated nanocomposite depends on the fraction of clay intercalated, f_i, and the fraction of clay exfoliated, $1 - f_i$. The mass fraction of the clay for intercalation based on the mass of composite is $\mu_c f_i$, and the volume of the intercalated clay tactoids can be calculated as

$$V^i = \frac{\mu_c f_i A[d_2(N-1) + h]}{N-1} \quad (19)$$

The volume of the exfoliated clay platelets is the volume of the exfoliated clay multiplied by the ratio of the thickness of platelets, h, to the basal plane spacing of the clay, d_1, as the interspacing is lost after exfoliation. Thus, it becomes

$$V_c^e = \frac{\mu_c(1 - f_i)Ah[d_1(N-1) + h]}{d_1(N-1)} \quad (20)$$

Neglecting the surface adsorption on the external surfaces of the intercalated clay, the volume of the interstitial polymer is the volume of the matrix of the exfoliated nanocomposite. Thus,

the volume of the polymer in the exfoliated nanocomposite is

$$V_p^i = \frac{1 - \mu_c - \mu_c f_i s}{\rho_p} \tag{21}$$

The volume of the exfoliated nanocomposite is

$$V^e = V_c^e + V_p^i \tag{22}$$

The total volume of the nanocomposite is

$$V = V^i + V^e \tag{23}$$

Thus, the volume fraction of the intercalated clay tactoids in the composite is given by

$$\frac{1}{\phi^i} = 1 + \frac{\rho_p A h \mu_c (1 - f_i)[d_1(N-1) + h] + d_1(N-1)(1 - \mu_c - \mu_c f_i s)}{\rho_p A d_1 \mu_c f_i [d_2(N-1) + h]} \tag{24}$$

The volume fractions of the subcomponents in the two nanocomposites can be also be found. If the specific volume of the composite is $1/\rho$, then the volume fraction of the intercalated clay tactoids can be found. In the case of organoclay, the volume of the intercalated clay tactoids is

$$V^i = \frac{\mu_c' f_i [d_2(N-1) + h]}{\rho_c' [d_1'(N-1) + h]} \tag{25}$$

The volume of the exfoliated clay platelets is

$$V_c^e = \frac{\mu_c'(1 - f_i)\mu_c^o}{\rho_c^p} \tag{26}$$

The volume of the composite $V = 1/\rho$; then the volume fraction of the intercalated clay tactoids is

$$\phi^i = \frac{\rho \mu_c' f_i [d_2(N-1) + h]}{\rho_c' [d_1'(N-1) + h]} \tag{27}$$

III. Reinterpretation of Elastic Modululi for Polymer−Clay Nanocomposites

A. Poly[oligo(ethylene glycol) diacrylate]−Clay Nanocomposites.[41] Modulus-nominal volume fraction data are available for these nanocomposites which were prepared by in situ polymerization. Their elastic moduli were obtained from ultrasonic pulse-echo testing. The volume fraction dependence of elastic moduli can be reinterpreted using effective volume fractions to acquire a more coherent picture of composite materials behavior.

From measurement of physical properties and from transmission electron microscopy (TEM),[41] $N = 8$, $A = 310$ m^2 g^{-1}, $d_2 = 1.73$ nm, and $\rho_p = 1220$ kg m^{-3}. The saturation ratio s was found to be 0.18 g g^{-1} clay and $h = 0.98$ nm. By inserting these data into eq 14, the nominal volume fractions of clay tested which were 0.017, 0.03, 0.13, 0.15, and 0.22 convert to 0.026, 0.045, 0.19, 0.22, and 0.32, respectively, which are the effective volume fractions of the reinforcement filler in the nanocomposites.

This allows existing volume fraction−elastic modulus models for composites (e.g., refs 4, 6, and 36−39) to be applied. In poly[oligo(ethylene glycol) diacrylate] (POEGDA)−clay nanocomposites, the reinforcement phase is the intercalated nanocomposite tactoids. The Poisson's ratio of montmorillonite was taken as 0.28 based on the literature values for mullite (0.28),[42,43] sillimanite (0.27),[42] kaolinite (0.27),[44] and montmorillonite (0.29).[44]

The elastic moduli of clay platelets have not been measured directly. Reasonable values have been assumed by others by selecting analogous minerals or have been calculated by numerical modeling. Unfortunately, these approaches present difference of a factor of 20.[45] Typical values that have been used by others (49,[46] 140,[47] and 178 GPa[48,49]) were taken as the Young's modulus of the clay platelets to study validity of volume fraction calculations. This represents the mid-range, neglecting the very low values of ~20 GPa[50] and the upper values deduced from molecular dynamic simulations of 400 GPa.[51]

Young's modulus and shear modulus for bulk polymer were measured using the ultrasonic pulse-echo method to be 2.8 GPa and 1.0 GPa. As discussed previously, the galleries hosted 0.18 g per g clay ($\mu_c^i = 0.85$). The density of the intercalated polymer can be calculated using eq 6, where $d_2 = 1.73$ nm, $h = 0.98$ nm, and $(A_T - A_P)/2 = 310$ m^2 g^{-1}, yielding $\rho_p^e = 759$ kg m^{-3}. This value is much lower than the density for the bulk polymer, 1220 kg m^{-3}. Two assumptions are made here for the elastic modulus of the intercalating polymer: one is to assume the intercalating polymer with density of 759 kg m^{-3} still exerts its bulk elastic moduli, 2.8 GPa for Young's modulus and 1.0 GPa for shear modulus; the other is to assume the intercalating polymer exerts its bulk density. In the latter case, the volume occupied is smaller than the interlayer spacing, producing a "porous structure" in the galleries which is expected to decrease the elastic modulus of the intercalated polymer. Clay platelets and a porous structure of polymer then form a sandwich foam structure.

According to Gibson and Ashby,[52] the Young's modulus of sandwich foam structures follows:

$$E_f = C E_s \left(\frac{\rho_f}{\rho_s}\right)^2 \tag{28}$$

where E_f and E_s refer to the Young's moduli of the foamed core and the solid structure. ρ_f and ρ_s refer to the densities of the foam and solid. C is a constant including all of the geometric constants of proportionality, and it approximates to unity.[52] For this system, $E_s = 2.8$ GPa, $\rho_f = 759$ kg m^{-3}, and $\rho_s = 1220$ kg m^{-3}; thus $E_f = 1.1$ GPa.

Christensen's equations for platelet-filled composites in the two-dimensional case[4,36] were used to calculate the elastic modulus of the clay tactoids. They provide

$$G = \frac{1}{h}(h_1 G_1 + h_2 G_2) \tag{29}$$

$$E = c_1 E_1 + c_2 E_2 + \frac{c_1 c_2 E_1 E_2 (\upsilon_1 - \upsilon_2)^2}{c_1 E_1 (1 - \upsilon_2^2) + c_2 E_2 (1 - \upsilon_1^2)} \tag{30}$$

where G is shear modulus, h is thickness of the alternating material, υ is Poisson's ratio, and c is volume fraction. Subscripts 1 and 2 refer to the clay and polymer, respectively. $h_1 = 0.98$ nm, $h_2 = 0.75$ nm, $\upsilon_1 = 0.28$, $\upsilon_2 = 0.39$, $E_2 = E_f = 1.1$ GPa, $c_1 = h_1/h$, and $c_2 = h_2/h$.

Substituting $E_1 = 49$, 140, and 178 GPa for eqs 29 and 30 gives $E = 28$ GPa and $G = 11$ GPa, $E = 80$ GPa and $G = 31$ GPa, and $E = 101$ GPa and $G = 40$ GPa, respectively. These

values vary less than 1 GPa compared to those calculated from the modulus for solid polymer using the same method. Thus, the elastic modulus for the intercalating polymer at reduced saturation in the galleries may not affect the modulus of the nanocomposite greatly because of the large gap between the modulus of the clay platelets and polymer.

Hashin−Shtrikman (H−S) bounds[53] are widely used (e.g., refs 54−57) and are often used to check the validity of new models or the interpretation of experimental data. For a two-phase material, the H−S lower and upper bounds for the effective bulk modulus (K_L and K_U) and shear modulus (G_L and G_U) are given by

$$K_U = K_1 + \frac{(K_2 - K_1)(1 - c_1)}{1 + (K_2 - K_1)c_1/\left(K_1 + \frac{4}{3}G_1\right)} \quad (31)$$

$$K_L = K_2 + \frac{(K_1 - K_2)c_1}{1 + (K_1 - K_2)(1 - c_1)/\left(K_2 + \frac{4}{3}G_2\right)} \quad (32)$$

$$G_U = G_1 + \frac{(G_2 - G_1)(1 - c_1)}{1 + 2(K_1 + 2G_1)(G_2 - G_1)c_1/5G_1\left(K_1 + \frac{4}{3}G_1\right)} \quad (33)$$

$$G_L = G_2 + \frac{(G_1 - G_2)c_1}{1 + 2(K_2 + 2G_2)(G_1 - G_2)(1 - c_1)/5G_2\left(K_2 + \frac{4}{3}G_2\right)} \quad (34)$$

Figure 3 shows that the experimental data fall between the H−S upper and lower bounds calculated from the three Young's moduli and are very close to the lower bounds when the platelet modulus is 140 or 178 GPa.

It is usual for the elastic modulus of reinforced composites to be close to the lower H−S bound (e.g., refs 58−62), especially at low reinforcement volume fractions. Hence, Figure 3 implies that the elastic modulus of nanocomposites can be interpreted using well-established theory provided that the effective reinforcement volume fraction is found.

B. Poly(ϵ-caprolactone)−Organoclay Nanocomposites. It is difficult to reinterpret the elastic moduli of intercalated polymer−clay nanocomposites from the open literature. The parameters required for the calculation of effective volume fractions such as the intercalation fraction of intercalated−exfoliated nanocomposites, the average number of clay layers per stack, the density of the organoclay, and the content of clay platelets in the organoclay are often lacking.

However, calculation of the effective volume fractions of reinforcement, i.e., the intercalated clay tactoids, is sometimes possible; poly(ϵ-caprolactone)−organoclay nanocomposites from Lepoittevin et al.[63] were selected for this calculation. The parameters to be applied into eq 17 are $N = 5$ (as determined from the TEM image), $d_2 = 2.77$ nm and $d_1' = 1.86$ nm (as determined from XRD patterns), $\rho_c' = 1870$ kg m^{-3}, $\rho_p = 1140$ kg m^{-3}, $\mu_c^\circ = 0.66$ for the organoclay, and s is assumed as 0.18 g g^{-1} clay. Thus, the effective volume fractions were calculated as 0.013, 0.040, 0.067, and 0.137 for clay platelet contents of 1, 3, 5, and 10 wt %, respectively.

The results of Young's modulus and effective volume fraction were plotted to give a comparison with the modulus vs the nominal volume fraction and are shown in Figure 4. The

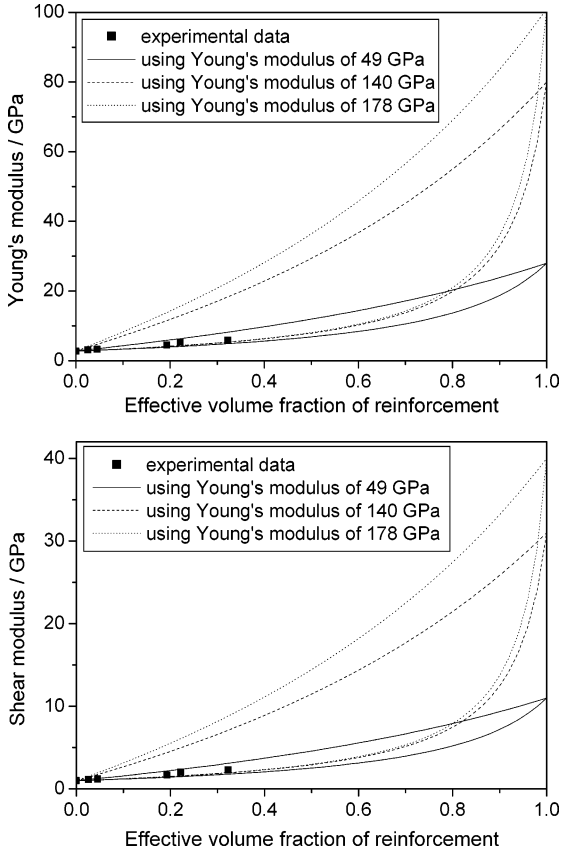

Figure 3. Elastic modulus vs effective volume fraction of reinforcement for poly[oligo(ethylene glycol) diacrylate]−clay nanocomposites[41] showing the experimental data fall within the Hashin−Shtrikman bounds at the three moduli of clay platelets tested.

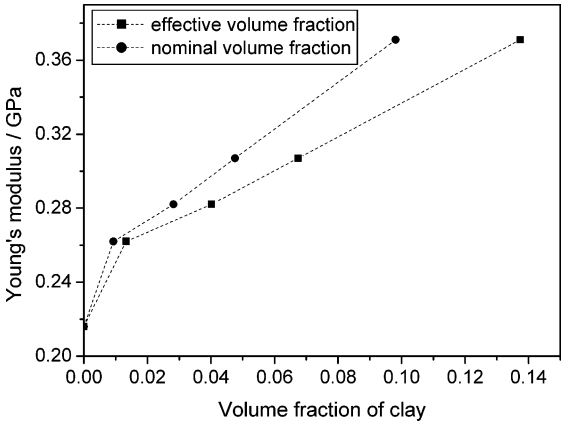

Figure 4. Young's modulus vs volume fraction of clay curves for poly(ϵ-caprolactone)−clay nanocomposites reported in the literature[63] showing the effective volume fractions are substantially greater than the nominal volume fractions.

effective volume fractions are much higher than the nominal volume fractions, being 41 ± 1% higher and confirming the need to use effective volume fractions for elastic modulus−volume fraction relationships.

IV. Conclusions

Systematic equations are presented for calculation of the effective volume fractions of the reinforcement in nanocomposites to include various types of configuration of reinforcement, namely intercalated nanocomposites, exfoliated nanocomposites, and intercalated−exfoliated nanocomposites.

For intercalated nanocomposites, the volume fraction of the true reinforcement filler is significantly greater than the volume

fraction of the clay particles. The elastic modulus of the reinforcement filler is also increased because the intercalating polymer has replaced the interlayer water which largely decreases the stiffness of the clay platelets. For exfoliated nanocomposites, clay platelets with high elastic modulus act as the reinforcement rather than the bulk clay particles. Also, the polymer layer adsorbed on the platelet surfaces is substantial due to the large surface area, which increases the effective volume fraction of the reinforcement. These help to explain the remarkable property enhancement in polymer−clay nanocomposites. The implication is that that the nanocomposites can actually be treated as a subset of conventional composites provided that the reinforcement is found correctly, and the effective volume fractions are properly calculated. Elastic modulus then follows the lower Hashin−Shtrikman bounds as it often does for conventional composites.

Acknowledgment. The Engineering and Physical Sciences Research Council is gratefully acknowledged for the financial support under Grant GR/T24166.

References and Notes

(1) Hull, D. *An Introduction to Composite Materials*; Cambridge University Press: Cambridge, 1981; p 3.
(2) Work, W. J.; Horie, K.; Hess, M.; Stepto, R. F. T. *Pure. Appl. Chem.* **2004**, *76*, 1985−2007.
(3) Hill, R. *J. Mech. Phys. Solids* **1965**, *13*, 213−222.
(4) Christensen, R. M. *Mechanics of Composite Materials*; John Wiley & Sons: New York, 1979; pp 46−48, 100−144.
(5) Sendeckyj, G. P. *Mechanics of Composite Materials*; Academic Press: New York, 1974; pp 55−77.
(6) Halpin, J. C. *Primer on Composite Materials: Analysis;* Technomic Publishing Co., Inc.: Lancaster, PA, 1984; pp 130−140.
(7) Cai, N.; Zhai, J.; Nan, C. W.; Lin, Y.; Shi, Z. *Phys. Rev. B* **2003**, *68*, 224103−1 − 7.
(8) Nielsen, L. *J. Macromol. Sci., Chem.* **1967**, *A1*, 929−942.
(9) Barrer, R. M. In *Diffusion in Polymers*; Crank, J., Park, G. S., Eds.; Academic Press: London, 1968; pp 165−216.
(10) Fan, Z. *Philos. Mag. A* **1996**, *73*, 1663−1684.
(11) Yano, K.; Usuki, A.; Okada, A.; Kurauchi, T.; Kamigaito, O. *J. Polym. Sci., Part A* **1993**, *31*, 2493−2498.
(12) Kojima, Y.; Usuki, A.; Kawasumi, M.; Okada, A.; Fukushima, Y.; Kurauchi, T.; Kamigato, O. *J. Mater. Res.* **1993**, *8*, 1185−1189.
(13) Lan, T.; Pinnavaia, T. J. *Chem. Mater.* **1994**, *6*, 2216−2219.
(14) Wang, Z.; Pinnavaia, T. J. *Chem. Mater.* **1998**, *10*, 3769−3771.
(15) Yano, K.; Usuki, A.; Okada, A. *J. Polym. Sci., Part A* **1997**, *35*, 2289−2294.
(16) Chen, B. *Br. Ceram. Trans.* **2004**, *103*, 241−249.
(17) Chen, B.; Evans, J. R. G. *J. Phys. Chem. B* **2004**, *108*, 14986−14990.
(18) Theng, B. K. G. *Formation and Properties of Clay-Polymer Complexes*; Elsevier Scientific Publishing Co.: Amsterdam, 1979; p 4.
(19) Shang, S. W.; Williams, J. W.; Soderholm, K. J. M. *J. Mater. Sci.* **1995**, *30*, 4323−4334.
(20) Bleach, N. C.; Nazhat, S. N.; Tanner, K. E.; Kellomaki, M.; Tormala, P. *Biomaterials* **2002**, *23*, 1579−1585.
(21) Ray, S. S.; Yamada, K.; Okamoto, M.; Fujimoto, Y.; Ogami, A.; Ueda, K. *Chem. Mater.* **2003**, *15*, 1456−1465.
(22) Chen, B.; Evans, J. R. G. *Macromolecules* **2006**, *39*, 747−754.
(23) Vaia, R. A.; Sauer, B. B.; Tse, O. K.; Giannelis, E. P. *J. Polym. Sci., Part B* **1997**, *35*, 59−67.
(24) Shen, Z.; Simon, G. P.; Cheng, Y.-B. *Eur. Polym. J.* **2003**, *39*, 1917−1924.
(25) Chen, B.; Evans, J. R. G. *Philos. Mag.* **2005**, *85*, 1519−1538.
(26) Granick, S.; Hu, H. W. *Langmuir* **1994**, *10*, 3857−3866.
(27) Peanasky, J.; Cai, L. L.; Granick, S.; Kessel, C. R. *Langmuir* **1994**, *10*, 3874−3879.
(28) Sens, P.; Marques, C. M.; Joanny, J. F. *Macromolecules* **1994**, *27*, 3812−3820.
(29) Helmy, A. K.; Ferreiro, E. A.; Bussetti, S. G. D. *J. Colloid Interface Sci.* **1999**, *210*, 167−171.
(30) Chen, B.; Evans, J. R. G. *Polym. Int.* **2005**, *54*, 807−813.
(31) Okada, A.; Usuki, A. *Mater. Sci. Eng., C* **1995**, *3*, 109−115.
(32) Lebaron, P. C.; Wang, Z.; Pinnavaia, T. J. *Appl. Clay Sci.* **1999**, *15*, 11−29.
(33) Aranda, P.; Ruiz-Hitzky, E. *Chem. Mater.* **1992**, *4*, 1395−1403.
(34) Kawasumi, M.; Hasegawa, N.; Kato, M.; Usuki, A.; Okada, A. *Macromolecules* **1997**, *30*, 6333−6338.
(35) Fornes, T. D.; Yoon, P. J.; Keskkula, H.; Paul, D. R. *Polymer* **2001**, *42*, 9929−9940.
(36) Christensen, R. M. *J. Eng. Mater. Technol.* **1979**, *101*, 299−303.
(37) Christensen, R. M. *J. Mech. Phys. Solids* **1990**, *38*, 379−404.
(38) Mori, T.; Tanaka, K. *Acta Metall.* **1979**, *21*, 571−574.
(39) Tandon, G. P.; Weng, G. J. *Polym. Compos.* **1984**, *5*, 327−333.
(40) Morgan, A. B.; Gilman, J. W. *J. Appl. Polym. Sci.* **2003**, *87*, 1329−1338.
(41) Chen, B.; Bowden, A. A.; Boulet, P.; Greenwell, H. C.; Coveney, P. V.; Whiting, A.; Evans, J. R. G. *J. Polym. Sci., Part B* **2005**, *43*, 1785−1793.
(42) Hildmann, B.; Ledbetter, H.; Kim, S.; Schneider, H. *J. Am. Ceram. Soc.* **2001**, *84*, 2409−2414.
(43) Ledbetter, H.; Kim, S.; Balzar, D. *J. Am. Ceram. Soc.* **1998**, *81*, 1025−1028.
(44) Vanorio, T.; Prasad, M.; Nur, A. *Geophys. J. Int.* **2003**, *155*, 319−326.
(45) Chen, B.; Evans, J. R. G. *Scr. Mater.*, in press.
(46) Fertig, R. S.; Garnich, M. R. *Compos. Sci. Technol.* **2004**, *64*, 2577−2588.
(47) Masenelli-Varlot, K.; Reynaud, E.; Vigier, G.; Varlet, J. *J. Polym. Sci., Part B* **2002**, *40*, 272−283.
(48) Kornmann, X.; Berglund, L. A.; Sterte, J.; Giannelis, E. P. *Polym. Eng. Sci.* **1998**, *38*, 1351−1358.
(49) Zhu, L.; Narh, K. A. *J. Polym. Sci., Part B* **2004**, *42*, 2391−2406.
(50) Ji, X. L.; Jing, J. K.; Jiang, W.; Jiang, B. Z. *Polym. Eng. Sci.* **2002**, *42*, 983−993.
(51) Sheng, N.; Boyce, M. C.; Parks, D. M.; Rutledge, G. C.; Abes, J. I.; Cohen, R. E. *Polymer* **2004**, *45*, 487−506.
(52) Gibson, L. J.; Ashby, M. F. *Cellular Solids: Structure and Properties*, 2nd ed.; Cambridge University Press: Cambridge, 1997; p 36.
(53) Hashin, Z.; Shtrikman, S. *J. Mech. Phys. Solids* **1963**, *11*, 127−134.
(54) Papadia-Einarsson, S. *Phys. Rev. B* **1997**, *55*, 10057−10063.
(55) Christensen, R. M. In *Mechanics of Composite Materials: Recent Advance*; Hashin, Z., Herakovich, C. T., Eds.; Pergamon Press: Oxford, 1982; pp 1−16.
(56) Tucker, C. L.; Liang, E. *Compos. Sci. Technol.* **1999**, *59*, 655−671.
(57) Wang, Z.; Wang, H.; Cates, M. E. *Geophysics* **2001**, *66*, 428−440.
(58) Peng, H. X. *Mater. Sci. Eng., A* **2005**, *396*, 1−2.
(59) Biswas, P.; Henshall, J. L.; Wakeman, R. J. *Mater. Sci. Eng., A* **1996**, *211*, 138−142.
(60) Wong, C. P.; Bollampally, R. S. *J. Appl. Polym. Sci.* **1999**, *74*, 3396−3403.
(61) Peng, H. X.; Fan, Z.; Evans, J. R. G. *Mater. Sci. Eng., A* **2001**, *303*, 37−45.
(62) Zhao, M.; Wu, G. H.; Dou, Z.; Zhang, L. T. *Mater. Sci. Eng., A* **2004**, *374*, 303−306.
(63) Lepoittevin, B.; Devalckenaere, M.; Pantoustier, N.; Alexandre, M.; Kubies, D.; Calberg, C.; Jerome, R.; Dubois, P. *Polymer* **2002**, *43*, 4017−4023.

MA0522460